A MULTIFRAME BAYESIAN ALGORITHM FOR DETECTING RANDOM SIGNATURE TARGETS IN CORRELATED GAUSS-MARKOV CLUTTER

Marcelo G. S. Bruno

Communications and Signals Lab (LCS)
Telecomm. and Control Depart., University of São Paulo
P.O. Box 61548, São Paulo SP 05424-970, Brazil
ph:(55-11) 818-5290; email:bruno@lcs.poli.usp.br

José M. F. Moura *

Laboratory for Information and Decision Systems
Massachusetts Institute of Technology, Room 35-203
77 Massachusetts Ave, Cambridge, MA 02139-4703 USA
ph: (617) 253-7250; email: moura@mit.edu

ABSTRACT

We introduce in this paper an optimal Bayesian algorithm for integrated detection and tracking of Gaussian targets that move randomly in cluttered environments. We model the background clutter as a noncausal Gauss-Markov random process and incorporate the statistical descriptions of the clutter, target signature, and target motion into the design of the detector/tracker. The optimal detection performance is quantified using Monte Carlo simulations.

1. INTRODUCTION

The problem we consider in this paper is to detect and track extended random signature targets that move randomly in heavily cluttered environments. The proposed solution is an optimal multiframe Bayesian algorithm that uses as data a sequence of sensor images and incorporates the statistical models for clutter, target signature and target motion. At each sensor scan, the algorithm decides whether targets are present or not and estimates the position of the targets that are declared present in the surveillance space. Detection and localization decisions are based on both current and previous sensor measurements using a recursive spatio-temporal data processing.

This paper extends to targets with random signatures the algorithm we had previously introduced for deterministic signature targets [1, 2, 3]. Section 2 reviews briefly the models for target signature, motion and clutter that underly our integrated approach to detection and tracking. Section 3 develops the optimal Bayes detector/tracker. In section 4, we detail the implementation of the algorithm in the particular case of spatially correlated Gaussian targets. We quantify the detection performance of the proposed Bayesian algorithm in section 5 using large-scale Monte Carlo simulations and compare it to the performance of the conventional single frame Neyman-Pearson detector. The results show that, in scenarios of dim targets/heavy cluuter, the multiframe Bayes detector significantly outperforms the traditional single frame schemes. Finally, section 6 summarizes the main contributions of the paper.

(*) On sabbatical leave from the ECE Department, Carnegie Mellon University, Pittsburgh, PA 15213-3890, USA.

2. THE MODEL

We review briefly in this section the models for target signature, target motion, and clutter statistics. For simplicity, we restrict ourselves to a scenario with one-dimensional (1D) surveillance spaces (e.g., radial motion with constant azimuth and elevation) and a single target per sensor scan with purely translational motion. The extension of the models to two-dimensional (2D) environments (targets that move randomly in a plane) is detailed in [1, 5].

Sensor Model

The sensor scans a bounded surveillance region which, given the sensor's finite resolution, is discretized by a uniform finite discrete lattice. Assuming a 1D surveillance region, the sensor lattice is an interval of the real line given by $\mathcal{L} = \{l: 1 \leq l \leq L\}$ where L is the number of resolution cells.

We introduce the random variable z_n that represents the target centroid position (range) in the sensor lattice during the nth sensor scan. In order to account for the situations when targets move in and out of the sensor range and in order to account for the possibility of absence of target, we define z_n on the *centroid lattice*

$$\overline{\mathcal{L}} = \{-l_s + 1 \leq l \leq L + l_i\} \tag{1}$$

where $(l_i + l_s + 1)$ is the maximum length of the 1D clutter free image of a possible target. From (1), we see that the centroid lattice includes all possible centroid positions for which at least one pixel of the target may be still present in the sensor image. Finally, in order to build an integrated framework for detection and tracking, we augment the centroid lattice with an additional dummy state that represents the absence of a target.

The final augmented lattice is

$$\tilde{\mathcal{L}} = \{l\colon -l_s+1 \leq l \leq L+l_i+1\} \qquad (2)$$

where $z_n = L + l_i + 1$ means that no target is present in the surveillance space during the nth sensor scan.

Target Model

Assuming real-valued sensor images, the clutter-free image of a possible target is a mapping

$$\begin{array}{rcl} \mathbf{f}\colon \tilde{\mathcal{L}} & \mapsto & \Re^L \\ z_n & \rightarrow & \mathbf{f}(z_n) \end{array} \qquad (3)$$

where

$$\mathbf{f}(z_n) = \sum_{k=-l_i}^{l_s} a_k^n \mathbf{e}_{z_n+k} \qquad z_n \in \overline{\mathcal{L}} \qquad (4)$$

$$\mathbf{f}(z_n) = \mathbf{0}_L \qquad z_n = L + l_i + 1 \, . \qquad (5)$$

In (4), $\mathbf{e}_l$, $1 \leq l \leq L$ is a vector whose entries are all zero, except for the lth entry which is one. If $l < 1$ or $l > L$, $\mathbf{e}_l$ is defined as the identically zero vector.

The coefficients $\{a_k^n\}$ are referred to as the target signature parmeters. In general, the target signature is time-variant and stochastic as a result of random changes in the reflectivity and/or conditions of illumination of the target. Let $\mathbf{a}_n = \left[a_{-l_i}^n \cdots a_{l_s}^n\right]^T$. In this paper, we assume that the sequence of random vectors $\{\mathbf{a}_n\}$, $n \geq 0$, is i.i.d. (independent, identically distributed) with a Gaussian probability density function $p(\mathbf{a}_n) = N(\mathbf{m}_a, \Sigma_a)$.

Observations and Clutter Model

The observations at the nth sensor scan, assuming a 1D surveillance region and a single target per frame, are collected in the L-dimensional column vector

$$\mathbf{y}_n = \mathbf{f}(z_n) + \mathbf{v}_n \qquad (6)$$

where $\mathbf{f}(z_n)$ is the nonlinear target model in (4) and (5), and $\mathbf{v}_n$ is the background clutter vector, also referred to as the background clutter frame. We assume that the clutter frames $\mathbf{v}_n$, $n = 0, 1, \ldots$, are also i.i.d.

Correlated Gauss-Markov clutter In general, each clutter frame $\mathbf{v}_n$ may exhibit a spatial (or intraframe) correlation. We capture the clutter's spatial correlation using the spatially homogeneous Gauss-Markov random field (GMrf) model [6]. The clutter vector, $\mathbf{v}_n$, is a zero-mean, finite order, noncausal, spatially homogeneous GMrf if it is the output, for $1 \leq i \leq L$, of the finite difference equation [6]

$$v_n(i) = \sum_{p=1}^{m} \alpha_p \left[v_n(i-p) + v_n(i+p)\right] + u_n(i) \qquad (7)$$

where $u_n(i)$ is a correlated zero-mean Gaussian input that is statistically orthogonal to $v_n(r)$, $\forall r \neq i$ and whose statistics we derive in the sequel. A set of boundary conditions is added to specify equation (7) near the boundaries of the lattice. In this paper, we assume Dirichlet boundary conditions, i.e., we make $v_n(i) = 0$, if $i < 1$ or $i > L$.

If we collect the samples $v_n(i)$ and $u_n(i)$, $1 \leq i \leq L$ in two long vectors $\mathbf{v}_n$ and $\mathbf{u}_n$, equation (7) can be written in matrix format as

$$\mathbf{A}\mathbf{v}_n = \mathbf{u}_n \qquad (8)$$

where $\mathbf{A}$ is a Toeplitz, symmetric, m-banded matrix with structure

$$\mathbf{A} = \mathbf{I} - \sum_{j=1}^{m} \alpha_j (\mathbf{K}_1^j + \mathbf{K}_2^j) \, . \qquad (9)$$

In equation (9), $\mathbf{I}$ is the L x L identity matrix and $\mathbf{K}_2$ is the L x L downward shift matrix whose entries are all zero, except for the elements $(i, i-1)$ which are equal to 1. $\mathbf{K}_1 = \mathbf{K}_2^T$ is the upward shift matrix. From the orthogonality condition and the assumption of spatial invariance in (7), we conclude that

$$E\left[\mathbf{v}_n \mathbf{u}_n^T\right] = \sigma_u^2 \mathbf{I} \Rightarrow E\left[\mathbf{u}_n \mathbf{u}_n^T\right] = \sigma_u^2 \mathbf{A} \qquad (10)$$

where $E\,[.]$ denotes the expected value and $\sigma_u^2 = E\left[u_n(i)\ v_n(i)\right]$, which is invariant with i by the spatial homogeneity assumption. Combining equations (8) and (10) and noticing the symmetry of $\mathbf{A}$, we see that

$$\Sigma_v = E\left[\mathbf{v}_n \mathbf{v}_n^T\right] = \sigma_u^2 \mathbf{A}^{-1} \qquad (11)$$

i.e., the covariance matrix of the clutter vector is proportional to the inverse of the structured matrix $\mathbf{A}$. We refer to $\mathbf{A}$ as the *potential matrix* [6]. A detailed study of the structure and eigendecomposition of the potential matrix for both 1D and 2D GMrfs and the relations between these models and fast sinusoidal orthogonal transforms is found in [4].

Motion Model

With translational motion, the motion of a target is completed specified by the dynamics of the target's centroid. The dynamics of the centroid the corresponding augmented lattice $\tilde{\mathcal{L}}$ is specified by a *transition probability matrix*, $\mathbf{T}$, whose general element $T(k, r)$ is

$$T(k,r) = \text{Prob}(z_n = k - l_s \mid z_{n-1} = r - l_s) \qquad (12)$$

where $1 \leq k, r \leq L + l_i + l_s + 1$.

3. OPTIMAL DETECTOR/TRACKER

Given the observations $\mathbf{y}_0^n = \left[\mathbf{y}_0^T\, \mathbf{y}_1^T \, \ldots \mathbf{y}_n^T\right]^T$, from instant 0 up to instant n, we want, at each instant n, to determine whether a target is present or not (detection) and, if the target is declared present, to estimate its position (range) in the surveillance space (tracking).

The optimal statistical solution for the joint detection/tracking problem follows a Bayesian strategy. From a Bayesian point of view, it suffices to compute at each instant n, the posterior probabilities $P(z_n \mid \mathbf{y}_0^n)$, for all possible values of the random variable z_n, including the absent state. The formal solution is divided into different steps.

Filtering Step Let $\bar{l} = l_i + l_s + 1$ and define the $\bar{l}$-dimensional column vector of signature parameters $\mathbf{a}_n$ such that

$$a_n(i) = a_i^n \qquad -l_i \leq i \leq l_s \ . \tag{13}$$

For $l_i + 1 \leq z_n \leq L - l_s$, the posterior probability of z_n conditioned on the observations is given by the expression

$$P(z_n \mid \mathbf{y}_0^n) = \int p(\mathbf{a}_n, z_n \mid \mathbf{y}_0^n)\, d\mathbf{a}_n \ . \tag{14}$$

In turn, using Bayes law and assuming that the sequence $\{\mathbf{v}_n\}$ is i.i.d. and independent of both $\{z_n\}$ and $\{\mathbf{a}_n\}$ for $n \geq 1$, we write

$$p(\mathbf{a}_n, z_n \mid \mathbf{y}_0^n) = C_n p(\mathbf{y}_n \mid \mathbf{a}_n, z_n) p(\mathbf{a}_n, z_n \mid \mathbf{y}_0^{n-1}) \tag{15}$$

On the other hand,

$$p(\mathbf{a}_n, z_n \mid \mathbf{y}_0^{n-1}) = p(\mathbf{a}_n \mid z_n, \mathbf{y}_0^{n-1}) P(z_n \mid \mathbf{y}_0^{n-1}) \ . \tag{16}$$

But, from the assumption that the sequence $\{\mathbf{a}_n\}$ is i.i.d. and independent of $\{z_n\}$ and $\{v_n\}$, for $n \geq 1$, we write

$$p(\mathbf{a}_n \mid z_n, \mathbf{y}_0^{n-1}) = p(\mathbf{a}_n) \ . \tag{17}$$

Using (17), equation (16) reduces to

$$p(\mathbf{a}_n, z_n \mid \mathbf{y}_0^{n-1}) = p(\mathbf{a}_n) P(z_n \mid \mathbf{y}_0^{n-1}) \ . \tag{18}$$

Substituting (18) into (15) and then, using (15) in (14), we conclude that

$$P(z_n \mid \mathbf{y}_0^n) = C_n \left[\int p(\mathbf{y}_n \mid \mathbf{a}_n, z_n) p(\mathbf{a}_n)\, d\mathbf{a}_n \right] \times P(z_n \mid \mathbf{y}_0^{n-1}) \ . \tag{19}$$

Note that, for $-l_s + 1 \leq z_n \leq l_i$ or $L - l_s + 1 \leq z_n \leq L + l_i$, equation (19) still holds, but the definition of $\mathbf{a}_n$ must be conveniently modified to account for portions of the target image that lie outside the sensor image.

Prediction Step From the total probability theorem

$$P(z_n \mid \mathbf{y}_0^{n-1}) = \sum_{z_{n-1}} P(z_n \mid z_{n-1}) P(z_{n-1} \mid \mathbf{y}_0^{n-1}) \ . \tag{20}$$

We detail in the sequel the minimum probability of error detector and the optimal MAP tracker.

Detector Let H_0 denote the hypothesis that no target is present at instant n and H_1 denote the hypothesis that a target is present during the nth sensor scan. Given $P(z_n \mid \mathbf{y}_0^n)$, compute the posterior probabilities of the detection hypothesis H_j, $j = 0, 1$. The minimum probability of error Bayes detector follows the decision rule

$$P(H_0 \mid \mathbf{y}_0^n) \underset{H_1}{\overset{H_0}{\gtrless}} P(H_1 \mid \mathbf{y}_0^n) \ . \tag{21}$$

Tracker If hypothesis H_1 is declared true, we compute the conditional probability vector

$$\begin{aligned} Q_l^f[n] &= P(\mathbf{z}_n = l \mid \text{target is present}, \mathbf{y}_0^n) \qquad l \in \overline{\mathcal{L}} \\ &= \frac{P(z_n = l \mid \mathbf{y}_0^n)}{1 - P(z_n = L + l_i + 1 \mid \mathbf{y}_0^n)} \end{aligned} \tag{22}$$

The MAP estimate of target's centroid position is

$$\hat{z}\text{map}[n] = \arg\max_{l \in \overline{\mathcal{L}}} Q_l^f[n] \ . \tag{23}$$

4. FILTERING STEP: CORRELATED GAUSSIAN TARGET

The challenge with random target signatures is to derive an analytic expression for the observations kernel

$$S_n(i) = \int p(\mathbf{y}_n \mid \mathbf{a}_n, z_n = i)\ p(\mathbf{a}_n)\ d\mathbf{a}_n \ . \tag{24}$$

Assume that the signature parameter vectors $\mathbf{a}_n$ is identically distributed for all sensor scans such that

$$p(\mathbf{a}_n) = p(\mathbf{a}) \qquad \forall n \ . \tag{25}$$

Suppose also that $\mathbf{a}$ is a Gaussian vector with mean $\mathbf{m}_a$ (different from zero) and covariance $\mathbf{\Sigma}_a$, and that the clutter vector $\mathbf{v}_n$ is an mth order noncausal GMrf as introduced in section 2. Under the assumption of GMrf clutter,

$$p(\mathbf{y}_n \mid \mathbf{a}, z_n = i) = k \exp(-\frac{\overline{Q}_i}{2\sigma_u^2}) \tag{26}$$

where k is a constant, $\overline{Q}_i$ is the quadratic form

$$\overline{Q}_i = \mathbf{y}_n^T \mathbf{A} \mathbf{y}_n - 2\mathbf{y}_n^T \mathbf{A} \mathbf{f}_i + \mathbf{f}_i^T \mathbf{A} \mathbf{f}_i \ . \tag{27}$$

In (27), $\mathbf{A}$ is the potential matrix from (9) and $\mathbf{f}_i = \mathbf{f}(z_n = i)$, with $\mathbf{f}$ being the nonlinear mapping in equations (4) and (5). Introduce now the vector

$$\mathbf{z}_n = \mathbf{A} \mathbf{y}_n \tag{28}$$

where

$$z_n(i) = y_n(i) - \sum_{j=1}^{m} \alpha_j \left[y_n(i+j) + y_n(i-j) \right] \qquad (29)$$

for $m+1 \leq i \leq L-m$. The term $z_n(i)$ in (29) is the error in the prediction of $y_n(i)$ by the *noncausal* (two-sided) mth order linear predictor

$$\hat{y}_n(i) = \sum_{j=1}^{m} \alpha_j \left[y_n(i-j) + y_n(i+j) \right] \ . \qquad (30)$$

For $1 \leq i \leq m$ or $L-m+1 \leq i \leq L$, boundary conditions must be supplied to define the predictor. We use *Dirichlet boundary conditions*, i.e, we make $y_n(k) = 0$ for $k < 1$ or $k > L$ and extend equation (29) to the entire range $1 \leq i \leq L$. We define in the sequel the $\bar{l}$-dimensional vector

$$\mathbf{z}_n^i = \left[z_{i-l_i}^n \ \dots \ z_i^n \ \dots \ z_{i+l_s}^n \right]^T \qquad l_i + 1 \leq l \leq L - l_s \ . \qquad (31)$$

Using now the results in [5], we write

$$\mathbf{z}_n^T \mathbf{f}_i = \mathbf{a}^T \mathbf{z}_n^i = \sum_{k=-l_i}^{l_s} a_k^n z_n(i+k) \qquad l_i+1 \leq i \leq L-l_s \ . \qquad (32)$$

On the other hand, also using the results from [5],

$$\mathbf{f}_i^T \mathbf{A} \mathbf{f}_i = E_f(0) - \sum_{j=1}^{m} \alpha_j (E_f(j) + E_f(-j)) \qquad (33)$$

for $l_i + m + 1 \leq L - l_s - m$. In (33),

$$E_f(0) = \mathbf{a}^T \mathbf{a} \qquad (34)$$

$$E_f(j) = \sum_{k=-l_i}^{l_s - j} a_k^n \, a_{k+j}^n \qquad (35)$$

$$E_f(-j) = \sum_{k=-l_i+j}^{l_s} a_k^n \, a_{k-j}^n \ . \qquad (36)$$

Notice that

$$E_f(j) = E_f(-j) = \mathbf{a}^T \mathbf{K}_1^j \mathbf{a} \qquad (37)$$

where $K_1(i,p) = 1$ if $p = i+1$, and zero otherwise, $1 \leq i, p \leq \bar{l}$. Hence,

$$\mathbf{f}_i^T \mathbf{A} \mathbf{f}_i = \mathbf{a}^T (\mathbf{I} - \sum_{j=1}^{m} 2\alpha_j \mathbf{K}_1^j) \mathbf{a} = \mathbf{a}^T \mathbf{\Sigma}_c \mathbf{a} \qquad (38)$$

for $l_i + m + 1 \leq L - l_s - m$, with

$$\mathbf{\Sigma}_c = \mathbf{I} - \sum_{j=1}^{m} 2\alpha_j \mathbf{K}_1^j \ . \qquad (39)$$

On the other hand, for $l_i + 1 \leq i \leq L - l_s$,

$$p(\mathbf{a}) = k_1 \exp \left[- \frac{(\mathbf{a} - \mathbf{m}_a)^T \mathbf{\Sigma}_a^{-1} (\mathbf{a} - \mathbf{m}_a)}{2} \right] \ . \qquad (40)$$

Combining all previous expressions, it follows that, for $l_i + m + 1 \leq i \leq L - l_s - m$,

$$S_n(i) = C \int \exp\left(\frac{1}{2} \left[2\sigma_u^{-2} \mathbf{a}^T \mathbf{z}_n^i - \mathbf{a}^T (\sigma_u^{-2} \mathbf{\Sigma_c}) \mathbf{a} - \mathbf{a}^T \mathbf{\Sigma}_a^{-1} \mathbf{a} + 2\mathbf{a}^T \mathbf{\Sigma}_a^{-1} \mathbf{m}_a \right] \right) d\mathbf{a} \ . \qquad (41)$$

where

$$C = k k_1 \exp\left(-\frac{\mathbf{y}_n^T \mathbf{A} \mathbf{y}_n}{2\sigma_u^2}\right) \exp\left(-\frac{\mathbf{m}_a^T \mathbf{\Sigma}_a^{-1} \mathbf{m}_a}{2}\right) \ . \qquad (42)$$

Completing the squares in (41), we notice that

$$\begin{aligned} 2\sigma_u^{-2} \mathbf{a}^T \mathbf{z}_n^i - \mathbf{a}^T (\sigma_u^{-2} \Sigma_c) \mathbf{a} - \mathbf{a}^T \mathbf{\Sigma}_a^{-1} \mathbf{a} + 2\mathbf{a}^T \mathbf{\Sigma}_a^{-1} \mathbf{m}_a &= \\ - \left[\mathbf{a}^T (\sigma_u^{-2} \Sigma_c + \mathbf{\Sigma}_a^{-1}) \, \mathbf{a} - 2\mathbf{a}^T (\sigma_u^{-2} \mathbf{z}_n^i + \mathbf{\Sigma}_a^{-1} \mathbf{m}_a) \right] &= \\ - \left[(\mathbf{a} - \mathbf{m}_i)^T \mathbf{\Sigma}_r^{-1} (\mathbf{a} - \mathbf{m}_i) - \mathbf{m}_i^T \mathbf{\Sigma}_r^{-1} \mathbf{m}_i \right] & \qquad (43) \end{aligned}$$

where

$$\begin{aligned} \mathbf{\Sigma}_r &= (\sigma_u^{-2} \Sigma_c + \mathbf{\Sigma}_a^{-1})^{-1} \\ \mathbf{m}_i &= \mathbf{\Sigma}_r \, (\sigma_u^{-2} \mathbf{z}_n^i + \mathbf{\Sigma}_a^{-1} \mathbf{m}_a) \ . \end{aligned} \qquad (44)$$

Integrating (41) and absorbing all constants into the normalization factor C_n, we finally write the ith entry of the observations kernel, $S_n(i)$, as

$$S_n(i) = \exp\left(\frac{\mathbf{m}_i^T \mathbf{\Sigma}_r^{-1} \mathbf{m}_i}{2}\right) \qquad l_i+m+1 \leq i \leq L-l_s-m \ . \qquad (45)$$

Remark: Boundary Conditions Near the boundaries of the lattice,we must modify the expressions for the observations kernel $S_n(i)$ in order to account for the fact that portions of the target are no longer visible in the sensor's image. For example, for $-l_s + 1 \leq i \leq l_i$, we get

$$\mathbf{y}_n^T \mathbf{A} \mathbf{f}_i = \mathbf{z}_n^T \mathbf{f}_i = \sum_{k=1-i}^{l_s} a_k^n z_n(i+k) = (\mathbf{a}_i^n)^T \mathbf{z}_n^i \qquad (46)$$

where

$$\mathbf{z}_n^i = \left[z_n(1) \dots z_n(i+l_s) \right]^T \qquad (47)$$

$$\mathbf{a}_i^n = \left[a_{1-i}^n \ \dots \ a_{l_s}^n \right]^T \ . \qquad (48)$$

Similarly, for $L - l_s + 1 \leq i \leq L + l_i$,

$$\mathbf{y}_n^T \mathbf{A} \mathbf{f}_i = \mathbf{z}_n^T \mathbf{f}_i = \sum_{k=-l_i}^{L-i} a_k^n z_n(i+k) = (\mathbf{a}_i^n)^T \mathbf{z}_n^i \qquad (49)$$

where

$$\mathbf{z}_n^i = [z_n(i - l_i) \ldots z_n(L)]^T \tag{50}$$

$$\mathbf{a}_i^n = \left[a_{-l_i}^n \ldots a_{L-i}^n\right]^T . \tag{51}$$

Likewise, the analytic expressions for the energy term $\rho_i = \mathbf{f}_i^T \mathbf{A} \mathbf{f}_i$ must changed to account for the correct length of the signature vectors $\mathbf{a}_i^n$. In order to compute the entries of the observations kernel, the procedure then is to write $p(\mathbf{y}_n \mid \mathbf{a}_i^n, \mathbf{z}_n = i)$, multiply it by

$$p(\mathbf{a}_i^n) = k_i \exp\left[-\frac{1}{2}(\mathbf{a}_i^n - \mathbf{m}_a^i)^T (\boldsymbol{\Sigma}_a^i)^{-1} (\mathbf{a}_i^n - \mathbf{m}_a^i)\right] \tag{52}$$

and complete the squares. The resulting expression for $S_n(i)$ is analogous to equation (45) with the proper corrections in the dimensions/definitions of the matrices and vectors used to compute $\mathbf{m}_i$ and $\boldsymbol{\Sigma}_r$. Another important point is that proper normalization factors must be used to make the normalization of $S_n(i)$ compatible with the normalization used away from the borders. We omit these technicalities here for the sake of conciseness.

5. DETECTION PERFORMANCE

We present in this section detection performance results for the algorithm introduced in section 3. We simulate 1D Gaussian targets with dimensions $l_i = l_s = 4$ moving in a grid of size $L = 100$. The simulated targets are samples of a correlated first GMrf model with mean $m_a = 1$ and covariance parameters α_a and σ_a. The target image is cluttered by a first order GMrf clutter with parameters α_c and σ_c.

We assume that there is at most one target present per frame. Targets that are present move in the sensor grid with nominal velocity of 2 pixels/frame and a probability of fluctuation of one pixel around the nominal position equal to 0.40. Once a target disappears from the grid, there is a total probability $p_a = 0.20$ of a new target reappearing randomly at any location in the sensor grid. This assumption corresponds to the worst case scenario when new tracks can be initialized with uniform probability at any cell in the sensor grid.

By varying the threshold in the detection test (21), the algorithm changes from a minimum probability of error Bayes test to a multiframe Neyman-Pearson test that maximizes the probability of detection for a fixed probability of false alarm. Figure 1 shows the experimental receiving operating characteristic curves (R0Cs) for the modified detector, with $\sigma_a = 0.2$, $\alpha_a = 0.16$, and $\alpha_c = 0.24$, for two levels of average SNR $= 20\log_{10}(m_a/\sigma_c)$, respectively 3 and 0 dB (i.e., $\sigma_c = 0.7$ and $\sigma_c = 1$). Figure 2 shows the ROCs now with $\sigma_a = 0.4$ (i.e, increasing the variance of the target pixels). The experimental curves were estimated from a total of 8,000 Monte Carlo runs.

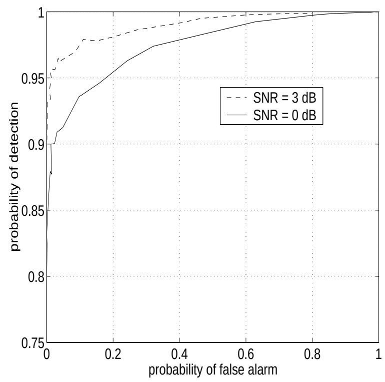

Figure 1: Multiframe Bayes detector in GMrf clutter, $\sigma_a = 0.2$

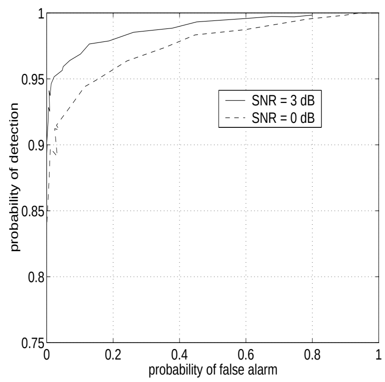

Figure 2: Multiframe Bayes detector in GMrf clutter, $\sigma_a = 0.4$

The plots in figures 1 and 2 indicate excellent detection performance, even in the adverse conditions of heavy clutter. For example, the algorithm reaches a 90 % probability of detection for false alarms rate of 10^{-3}. There is a slight perceptible deterioration within the margin of error of the experiment when we increase the target variance.

We compare in the sequel the optimal multiframe detector with a single frame likelihood ratio test (LRT) that ignores the motion model. The single frame LRT algorithm reduces to the test

$$p(\mathbf{y}_n \mid H_0) \underset{H_1}{\overset{H_0}{\gtrless}} \lambda\, p(\mathbf{y}_n \mid H_1) \tag{53}$$

where λ is a threshold that varies according to the desired probability of false alarm. Using a fixed value of

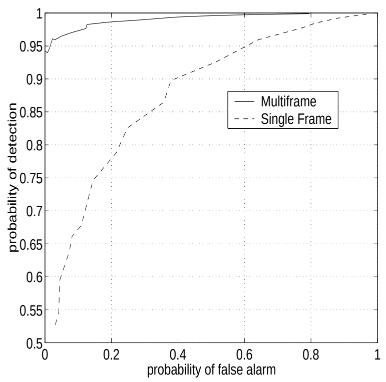

Figure 3: Single frame versus multiframe ROCs in correlated clutter: $\sigma_a = 0.2$ and $\sigma_c = 0.7$

SNR, we vary the thresholds in tests (21) and (53) to plot the receiver operating characteristic curves (ROCs) for both detectors. The ROC curves, estimated from 8,000 Monte Carlo runs, are shown in figure 3 for SNR $= 3$ dB and $\sigma_a = 0.2$. The curves in figure 3 show that, in a scenario of dim targets, there is a dramatic deterioration in performance if detection decisions are made based on one single frame, ignoring the motion model. These results corroborate the advantages of spatio-temporal processing in moving targets detection.

6. SUMMARY

We presented in this paper an optimal Bayesian algorithm for multiframe detection and tracking of moving correlated Gaussian targets in correlated Gauss-Markov clutter. Performance studies using Monte Carlo simulations show that there is a substantial detection performance improvement over the single frame likelihood ratio test (LRT) detector.

ACKNOWLEDGEMENT

This work was funded by FAPESP, São Paulo, Brazil. The work of the second author was partially funded by ONR grant N00014-97-1-0800.

7. REFERENCES

[1] Marcelo G. S. Bruno and José M. F. Moura. "The Optimal 2D Multiframe Detector/Tracker". *AEÜ International Journal of Electronics and Communications*, 53(6), pp. 346-355, December 1999.

[2] Marcelo G. S. Bruno and José M. F. Moura. "Performance of the Optimal Nonlinear Detector/Tracker in Clutter". *Proceedings IEEE ICASSP'99*, pp. 1193-1196, Phoenix AZ, March 15-19, 1999.

[3] Marcelo G. S. Bruno and José M. F. Moura. "Optimal Multiframe Detection and Tracking in Digital Image Sequences". *Proceedings IEEE ICASSP'2000*, Istanbul, Turkey, June 5-9, 2000.

[4] José M. F. Moura and Marcelo G. S. Bruno. "DCT/DST and Gauss-Markov Fields: Conditions for Equivalence". *IEEE Transactions on Signal Processing*, 46(9), pp. 2571-2574, September 1998.

[5] Marcelo G. S. Bruno. *Joint Detection and Tracking of Moving Targets in Clutter*. Ph.D. Thesis, ECE Department, Carnegie Mellon University, 1998.

[6] José M. F. Moura and Nikhil Balram. Recursive Structure of Noncausal Gauss Markov Random Fields. *IEEE Transactions on Information Theory* IT-38(2): 334-354, March 1992.